PAPER

Laser isotope separation scheme of lithium by three-color photoionization

IOP Publishing Physica Scripta
Phys. Scr. 95 (2020) 075403 (10pp) https://doi.org/10.1088/1402-4896/ab94d8

Laser isotope separation scheme of lithium by three-color photoionization

V K Saini[1,2], S Talwar[3], V V V Subrahmanyam[4], R K Mishra[5], P K Saini[2] and S K Dixit[1,2]

[1] Homi Bhabha National Institute, Training School Complex, Anushakti Nagar, Mumbai 400094, India
[2] Fibre Sensors and Optical Spectroscopy section, Raja Ramanna Centre for Advanced Technology, Indore 452013, India
[3] Laser Controls and Instrumentation Division, Raja Ramanna Centre for Advanced Technology, Indore 452013, India
[4] Advanced Lasers and Optics Division Raja Ramanna Centre for Advanced Technology, Indore 452013, India
[5] Laser Power Supplies Division, Raja Ramanna Centre for Advanced Technology, Indore 452013, India

E-mail: vksaini@rrcat.gov.in

Received 26 March 2020, revised 28 April 2020
Accepted for publication 20 May 2020
Published 28 May 2020

Abstract

Lithium isotopes (^{6,7}Li) are of prime importance for nuclear industry. Especially, highly enriched ^{6}Li is needed in fusion reactors to produce clean energy on large scale. In this paper, we report studies on Li isotope separation by isotope-selective three-color photoionization using 'kHz' repetition rate narrowband dye lasers in conjunction with time-of-flight mass spectrometer. The method established yields a high degree of selectivity by tuning the dye lasers to respective ^{6,7}Li resonance levels and demonstrated the enhancement of low abundant (7.5%) ^{6}Li up to 92.86% at signal level. The dependence of photo-ionization yield, isotope selectivity and abundance enhancement on laser powers are also investigated. The proposed photo-ionization scheme [$^{2}S_{1/2} \rightarrow \xrightarrow{\sim 671\ nm} {}^{2}P_{1/2,3/2} \rightarrow \xrightarrow{\sim 610\ nm} {}^{2}D_{3/2,5/2} \xrightarrow{\sim 578\ nm} {}^{1}S_{0}$ (Li^{+})] enables the high photo-ionization yield and large enhancement (>12 fold) in ^{6}Li abundance.

Keywords: Lithium, resonance ionization, dye laser, mass-spectrometer, laser isotope-enrichment

(Some figures may appear in colour only in the online journal)

1. Introduction

Lithium has two stable isotopes ^{6}Li (7.5%) and ^{7}Li (92.5%). The highly enriched ^{6}Li (>90%) is needed to produce the clean energy on vast scales through (D-T) nuclear reaction in fusion reactors. The deuterium (D) is commercially available in large quantities; however, the tritium (T) is not a primary fuel and has to breed inside the reactor blanket itself. The enriched ^{6}Li with large thermal neutron cross-section (~940 barns) is a good source of tritium and can be used as a fuel in fusion reactors [1]. Adequate tritium can be produced artificially by ^{6}Li (n, α) T reaction, as its natural abundance found among hydrogen isotopes is too low to fulfill the present needs. Today, the worldwide rechargeable battery market is dominated by lithium-ion batteries. The use of ^{6}Li-enriched electrolyte in lithium-ion batteries is also an important and current topic of research [2]. Therefore, study on selective photoionization of lithium for laser-based separation/enrichment of its isotope is important. For better clarity on text, the acronyms used are listed in table 1.

Numerous methods have been tried over long period to separate and enrich the Li isotopes. Most often, the chemical separation methods such as an ion exchange, Li/Hg amalgam chemical exchange or electrolysis (mercury-cathode) etc being used. These methods undoubtedly offer higher yield; however, limited by a low separation factor and high toxicity [3]. The physical methods (e.g. gas diffusion or centrifuge) are mostly dependent on mass difference in isotopes and usually suitable for heavy elements. Laser isotope separation (LIS) is equally applicable for light and heavy mass elements

Table 1. Nomenclature of the acronyms used.

Words	Acronyms	Words	Acronyms
Lithium	Li	Copper vapor laser	CVL
Deuterium	D	Master-oscillator/ power-amplifier	MOPA
Tritium	T	4-(Dicyanomethylene) -2-methyl-6-(4-dimethylaminostyryl)-4H-pyran	DCM
Laser isotope separation	LIS	Dimethyl sulfoxide	DMSO
Time-of-flight	TOF	Isotope enhancement factor	IEF
Mass-spectrometer	MS	Amplified spontaneous emission	ASE
Resonance ionization spectroscopy	RIS	Hyperfine fine structure	HFS

and differs fundamentally from gas diffusion/centrifuge methods. The LIS distinguish isotopes of an element through precise differences in their electronic structures. The energy levels scheme of isotopes is different either due to difference in their reduced masses and/or difference in nuclear charge distribution. These differences (isotopic shift, hyperfine structure) are small; however, affect the energy levels of isotopes and their excitation energy, considerably. Therefore, each isotope absorbs a light of slightly different wavelengths. As the lasers are highly monochromatic and intense in nature, so these can be used to excite or pick a specific single isotope leaving all others undisturbed. As quantum mechanics states that an atom can absorb the photons energy in discrete units only, that's why the atom is considered to have only finite number of discrete energy levels, each one representing a particular electronic configuration. The light can be absorbed by atoms only when incident photons exactly fill the energy gap in between two quantum mechanically allowed energy states. The absorbed photon induces the change in atom electronic configuration with the valence electron promoted into higher energy states reaching the atom in excited state. Additional photons of an appropriate energy can further excite the atom to higher energy levels. The ultimate limit is an ionization level where the electron becomes free and atom gets ionized. The LIS is very attractive in terms of high selectivity and isotope purity. As compared to diffusion/centrifuge methods, the LIS is cost-effective with a smaller number of stages to attain the same isotopic enrichment factor and less toxic than chemical methods.

In LIS method, a specific isotope is selectively excited using narrowband tunable laser keeping other isotopes in ground state. Further, the excited isotope gets ionized by other photons of suitable energy. The resulting photo-ions of desired isotope can be extracted by applying an electric and/or magnetic field. Here, the spectral bandwidth of tunable laser is required to be smaller than isotopic shift to obtain the high selectivity and isotope purity. The overall selectivity can be increased further by multi-step excitation/ionization of a well collimated atomic beam using narrowband dye lasers with moderate output power. The large power density from lasers may affect the selectivity due to power broadening of atomic transitions and/or multiphoton ionization that may lead to loss in isotopic enrichment [4]. On the other hands, large power densities are beneficial to high photo-ionization yield. Therefore, simultaneous optimization of isotope selectivity and ionization-yield are of prime importance in LIS enrichment method.

Resonance ionization spectroscopy (RIS) is considered to be the most useful tool for LIS that needs tunable laser sources with line-width narrower than transition isotopic-shift [5, 6]. The pulsed laser system facilitates the simplest and efficient coupling of time-of-flight mass-spectrometer (TOFMS) to RIS to investigate the desired mass isotopes. Alkali metals have been studied extensively by two-step photo-ionization as well as isotope-selective chemical reaction schemes using the narrowband tunable lasers [7–9]. Karlov *et al* [10] demonstrated an applicability of two-step RIS process for isotope separation of rare earths such as neodymium (Nd), samarium (Sm), europium (Eu), gadolinium (Gd), dysprosium (Dy) and erbium (Er). In recent, Locke *et al* [11] carried out selective photoionization of palladium (Pd) isotopes using two-step excitation method to recycle the Pd occurring in nuclear waste. Il'in *et al* [12] studied the Li isotopes photoionization in two frequency laser field using TOFMS and ionizing radiation of 266 nm. Saleem *et al* [13] reported Li two-step photoionization and obtained 47% enhancement in ^{6}Li abundance. Recently, author has reported studies on Li isotope separation by two-step photo-ionization scheme using low repetition rate (∼Hz) and nanosecond (∼ns) lasers [14], wherein main focus was on measurements of relative Li isotopic ratio and their photo-ionization cross-section. A moderate ^{6}Li abundance enhancement limited up to 72% was also obtained. Now, we report on Li three-color isotope-selective photoionization using in-house built system such as high repetition rate copper vapor laser (CVL) pumped dye lasers and TOFMS. In present work, we focused on the studies of dependence of photo-ionization yield, isotope selectivity and abundance enhancement on laser powers in context to laser isotope enrichment of Li. A very large enhancement in ^{6}Li abundance up to 92.86% is achieved for isotope selectivity (∼160).

2. Experimental setup

Figure 1 shows a schematic view of an experimental setup we used to realize three-color photoionization for Li isotope separation. The setup consists of high repetition rate CVL in master-oscillator/power-amplifier (MOPA) configuration, pulsed tunable dye lasers, Li atomic beam source (oven), dye laser tuning electronics (not shown here), TOF mass-

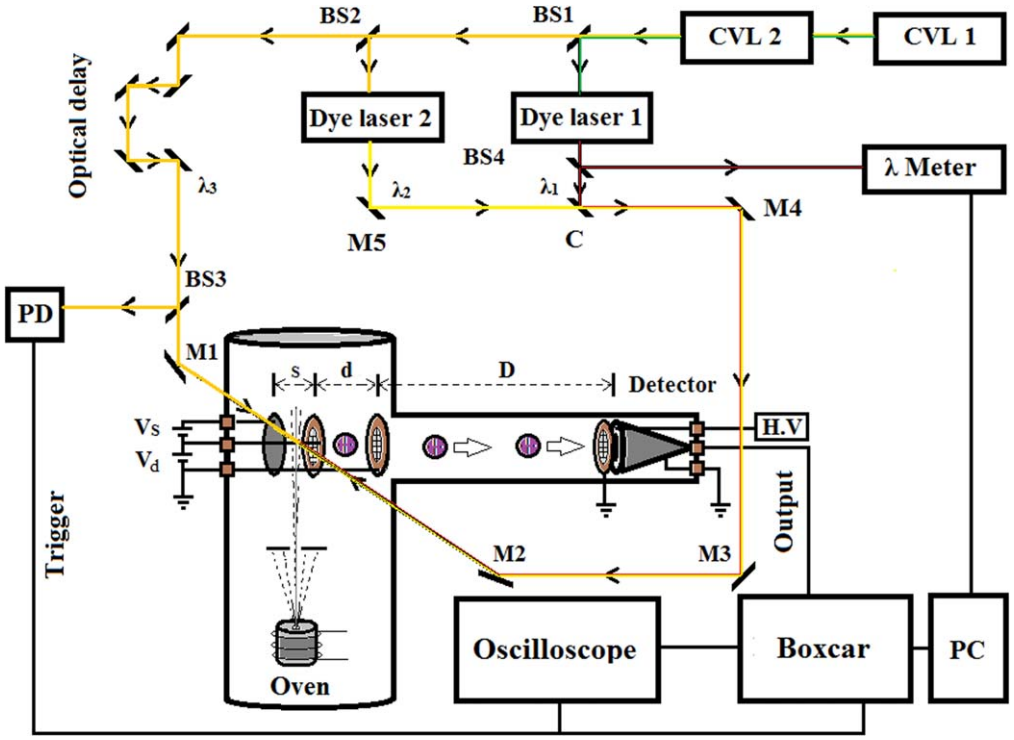

Figure 1. Schematic of three-color isotope-selective photoionization for Li isotope separation. (1). CVL-1 (Oscillator, 20 W) (2). CVL-2 (Amplifier, 35 W) (3). Dye laser-1 (2.5 GHz, 20 ns, 630–675 nm, 2.6 mM) (4). Dye laser-2 (2.5 GHz, 20 ns, 600–625 nm, 0.16 mM) (5). λ-meter (WS-7, HighFinesse/Ångstrom) (6). Boxcar Integrator (SRS-250) (7). Oscilloscope (Lecroy, 500 MHz) (8). PD: Si-Photodiode 9. PC: Personal computer 10. TOF parameters: ionization region (s = 8 mm), acceleration region (d = 35 mm), field free flight region (D = 1200 mm), detector: Channeltron KBL 25 operated @−2.0 kV 11. Typical λ_1, λ_2, λ_3: (671, 610, 578 nm).

spectrometer, and PC-based data acquisition. The CVL has an advantage as it emits the green (510.5 nm) and yellow (578.2 nm) colour beams with good quality simultaneously, suitable to pump the two dye lasers used for successive Li transitions. The yellow beam emits with a delay of few nanoseconds after the green pulse. The CVL can operate at high repetition rate (∼6.5 kHz) with short pulse duration (∼40 ns) which is useful for higher photo-ionization yield in LIS setups. It can be operated at energies of several mJ/pulse. Its energy can be increased further by operating CVL in MOPA configuration.

Both the pump laser as well as tunable dye lasers used in the present study, are developed in-house [15]. The dye laser-1 unit used for Li 1st_step resonant excitation consists of an oscillator and amplifier with output power of 550 mW at ∼671 nm. A flowing type of homemade dye-cell [16] fabricated from BK-7 material fitted in stainless steel frame is used for both the dye laser-1 and dye laser-2 units. The dye laser-2 consists of an oscillator part only. A well-known Littman type dye laser resonator geometry with grating mounted in grazing incidence mode is used to obtain a narrow linewidth output [17]. The DCM [4-(dicyanomethylene)-2-methyl-6-(4-dimethylaminostyryl)-4H-pyran] dye dissolved in dimethyl sulfoxide (DMSO) solvent serves as gain media for both the oscillator as well as amplifier to obtain the tunable laser output across 671 nm. The DCM dye in DMSO solvent has good absorption at CVL 510.5 nm radiation. The concentration of dye solutions for oscillator and amplifier are adjusted as 2.6 and 1.2 mM, respectively for optimum output at 671 nm in the spectral range of 635 to 680 nm. The oscillator and amplifier are pumped by the CVL green (510.5 nm) component of 3.5 and 10 W, respectively using the cylindrical lenses each of focal length (+10 cm). For more clarity, schematic and layout of dye laser-1 oscillator part is shown in figure 2.

The resonator of oscillator consists of a holographic grating (2400 l mm^{-1}), plane reflecting (R ∼100%) tuning mirror, wedged output coupler with 20% reflection coating and an intra-cavity double prism beam-expander of magnification (M = 20) inclined at 85° of incidence angle. The cavity length is restricted minimum (∼15 cm). The conversion efficiency of oscillator is around 2%. The output from oscillator is focused by a convex lens (f = 50 cm) into the amplifier dye-cell after spatial filtering using a pinhole (∼500 μm) to minimize the amplified spontaneous emission (ASE). In this way, high average power of 550 mW at 6.5 kHz is obtained at 671 nm. The bandwidth (∼2.5 GHz) of dye laser-1 is measured using a high precision (HighFinesse, WS-7) wavelength (λ) meter. In similar way, another tunable dye laser-2 (∼2.5 GHz, 20 ns, Rh-640 dye, 0.16 mM, 150 mW, 600–625 nm) is developed for Li 2nd_step of resonant excitation. It simply consists of an oscillator part which is pumped by the CVL-MOPA yellow output (578.2 nm). These dye lasers can be scanned over their full tuning range by changing the angle of tuning mirror using a picomotor actuator (Newport, model: 8302) with a resolution of 30 pm/step. Such

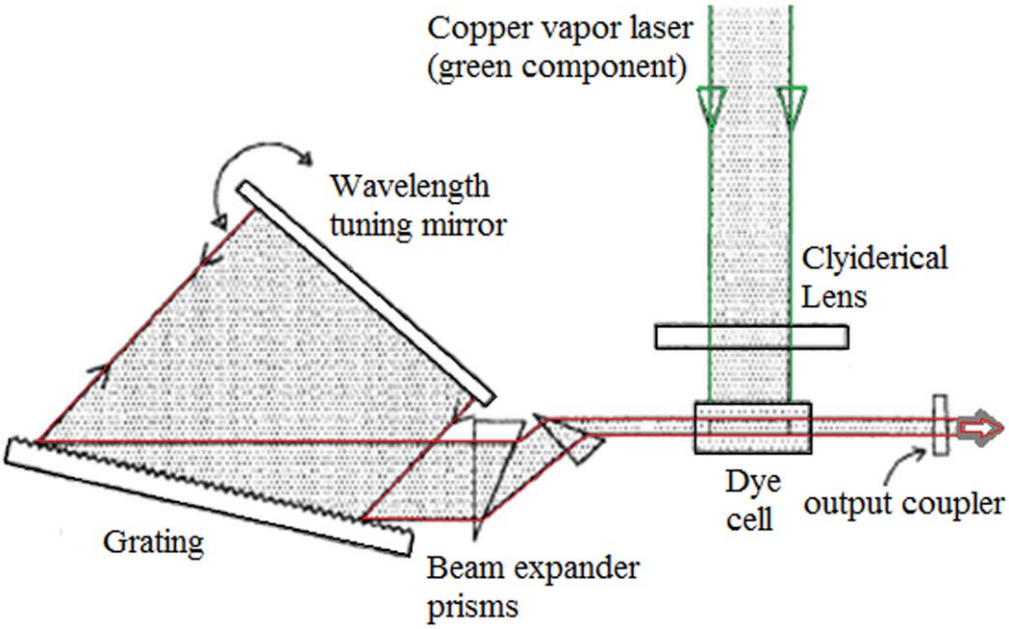

Figure 2. Schematic of an oscillator part of dye laser-1 for Li 1st resonant excitation.

tunable dye lasers are important for the selective-photo-ionization experiments and laser isotope separation [18, 19].

In this experimental setup, a dichoric mirror BS1 is used to separate green and yellow components of CVL output radiation to pump the respective dye lasers. The components BS2 to BS4 are the partial beam splitters. The beam combiner 'C' is used to merge the dye laser-1 and dye laser-2 outputs tuned at wavelengths λ_1 and λ_2 corresponding to Li first and second step of excitation, respectively. These wavelengths are monitored by high precision λ-meter (WS-7). The reflecting mirrors M1 to M5 ($R > 99\%$) guides the respective lasers output into TOF ionization chamber where they interact with collimated Li atomic beam. The details of atomic beam oven are described in the next section. An optical delay line provides the desired excitation delay to the third-step of Li photo-ionization. The output from fast Si photo diode (PD) is used as a trigger for oscilloscope as well as boxcar integrator (SRS-250). The boxcar integrator consists of a gate generator, a fast-gated integrator and an exponential averaging circuitry. The boxcar integrator is an instrument of choice for the recovery of repetitive and small duty cycle weak signals such as in the present experiment. Here, the TOF mass-spectrometer output is processed through boxcar that filters out the noise from ionization signal and retrieved on personal computer (PC).

3. Li atomic beam source

To minimize Doppler broadening effect, a well collimated Li atomic beam vertical to laser beam interaction is generated by resistive heating mechanism. For that, an atomic vapour source having cylindrical oven of 12 mm inner diameter and volume 2800 mm^3 that can occupy $\sim$1.5 gm of Li is developed. It is made of corrosion resistant high-quality stainless

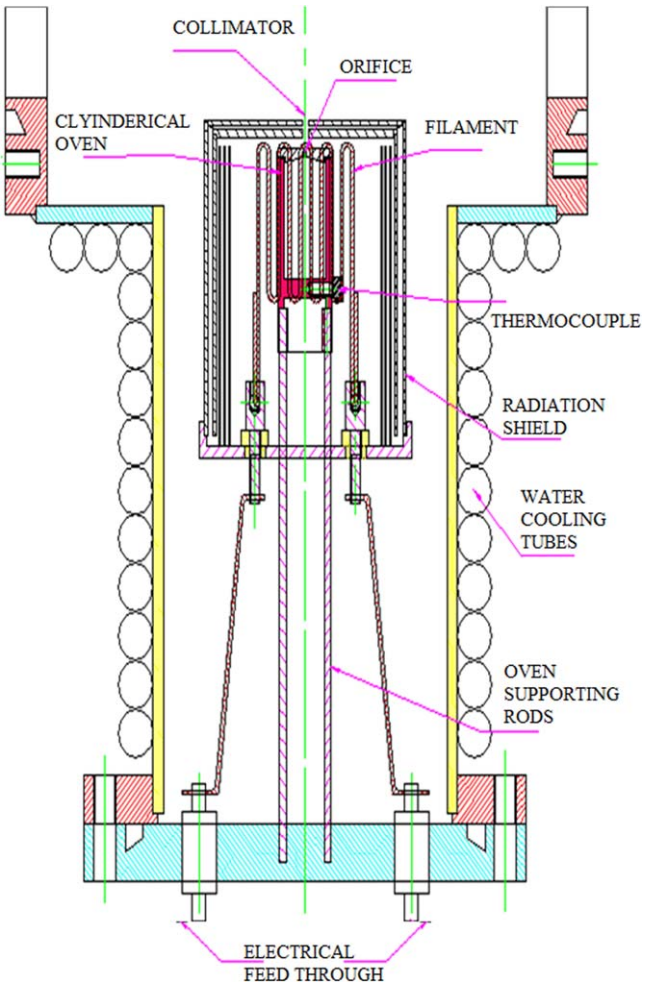

Figure 3. Schematic of Li atomic beam source.

steel (316 SS). The design of atomic beam source (figure 3) is kept compact and adaptable to TOF mass spectrometer. It can be detached easily from its ion source to reload the Li sample.

The atomic source is installed just beneath ionization/extraction region of mass-spectrometer. The temperature of Li atomic gas is monitored *in situ* using a thermocouple (K type) directly mounted on oven surface. The small fluctuations in atomic flux are cared with precise PID (proportional–integral–derivative controller) control of heating current to maintain the temperature of atomic oven within $\pm$ 1 °C. To minimize radiative heat losses, the oven is surrounded by thin multi-layer molybdenum radiation shields. The atomic beam is emerged through an exit hole of 1 mm diameter. At an operating temperature 525 °C reached with tantalum filament current of 16 A, the calculated mean free path ($L = 1/n\sigma \approx 24$ cm) is found much higher than exit hole diameter (1 mm) that ensures transparent flow of Li atoms without collisions. To suppress the possibility of any thermal electron/ion emission that otherwise may register an undesired background event on TOF ion-detector, the oven jacket is externally cooled by flowing water into copper cooling tubes. The atoms effuse out at an average speed of 1.35×10^5 cm s^{-1} through oven exit hole and the rate is estimated to be 3.7×10^{16} atoms per second. The atom density generated inside oven is estimated from its temperature and available Li vapor pressure curves. The temporal and spatial overlap of atomic beam with laser beams are main limiting factors that may restrict overall efficiency of RIS coupled TOF system. The temporal overlap can be determined by a fraction

$$F_t = d_L \nu_{rep} / \bar{v} \quad (1)$$

where d_L is the diameter of laser beam in interaction region, ν_{rep} the laser pulse repetition rate and $\bar{v}$ the average thermal speed of atoms. Hence, pulse repetition rate of CVL ($\nu_{rep} = 6.5$ kHz), $\bar{v} = 1.35 \times 10^5$ cm s^{-1} and $d_L \sim 1$ mm for Li at 525 °C contribute a temporal fraction $F_t = \sim 0.005$. Similarly, spatial overlap can be calculated as

$$Fs = (\kappa/\pi)\Delta\Omega \quad (2)$$

where Fs is fraction of the atoms entering into laser interaction region within solid angle $\Delta\Omega$ at $\theta \approx 0^0$. Factor κ depends upon source geometry and θ is the angle with beam limiting diaphragm symmetry axis. For effusion of atoms from long channel ($l = 25$ mm, r = 0.5 mm) of oven, the number of atoms evaporated into solid angle ($\Delta\Omega$) increases by a factor $\kappa = 3l/8r$ [20]. For an interaction region of area d_L x s (where s = FWHM of atomic beam, and $s \geqslant d_L$) at distance 'b' from atomic source, the fraction of atoms entering into interaction zone is

$$Fs = (\kappa/\pi)[d_L s/\pi b^2] \quad (3)$$

For typical setup values ($d_L = 1$ mm, s = 5 mm, b = 5 mm and $\kappa = 18.7$), Fs is ~0.012. In this way, total fractional value is $F_{tot} = Fs \times F_t \approx 5.7 \times 10^{-5}$ that gives an overall atom density into laser interaction zone as $\sim 2.1 \times 10^{12}$ atoms/cm^3.

In present setup, an in-house developed linear TOF mass-spectrometer with mass resolution ($m/\Delta m \sim 23$) similar to that developed by Talwar *et al* [21] is used. Such mass-spectrometers are very useful in spectroscopic studies, trace analyses and ionic mass to charge (m/z) ratio measurements [22–25]. Though different kinds of mass-spectrometers are customary now-a-days, still the TOF mass-spectrometer is an instrument of choice for resonance photoionization studies due to its easier coupling with pulsed laser system and simpler in design. More details of the same are described elsewhere [14]. The photo-ion current from TOFMS ion-detector is measured directly on digital oscilloscope which is triggered by a laser pulse using fast Si photodiode. The photo-ion current signal is optimised with respect to the delays between first (red), second (yellow) resonant step exciting laser beams and third non-resonant ionizing laser beam. Suitably delayed (~5 ns) ionizing laser pulse appears just after an exciting laser pulse to extract the maximum population available in excited states before decaying to ground state to obtain the higher photoionization efficiency for each isotope. The output signal is averaged over 100 acquisitions by boxcar integrator (SRS-250) to compensate the effects of pulse-pulse laser energy variation on photo-signal.

4. Three-color photoionization scheme for Li

The photoionization of Li atoms can be carried out through different energy pathways whose common feature is selective excitation of one or more intermediate atomic states followed by the subsequent ionization of excited atoms either by an additional laser radiation, electric field or through collisions with other particles [5, 6]. The simplest one is the two-step photoionization in the absence of external fields or collisions; however, the selectivity remains limited if auto-ionization levels are absent and such is the case with Li [11–13]. Higher selectivity can be obtained through multi-step resonant excitation, in which number of intermediate steps involved is decided by the ionization potential (I.P) of element and the photons energy of laser radiation used. Higher the number of resonant intermediate atomic states more is the selectivity of process [26]. However, resonant transfer of energy from excited isotope to the unexcited ones may limit the selectivity of multistep photoionization process [27]. In such cases, the decrease in selectivity can be overcome by limiting atom density ($\leqslant 10^{12}$ cm^{-3}) [26]. The isotope selectivity and photoionization efficiency both depend upon available resonance ionization transitions and the energy pathways selected [6]. In this process, isotope-shift of atomic transitions is particularly one of the dominating factors that determine the isotope selectivity which need to be optimized for each excitation steps. Theoretical isotope selectivity (S) can be defined as

$$S = [2\Delta\nu/\Gamma_{nat.}]^2 \quad (4)$$

where Γ_{nat} is the natural linewidth and $\Delta\nu$ the isotope-shift of a specific transition. Ideally, the photoionization schemes that comprise the atomic transitions with large isotopic shift, small natural linewidth and of course with non-overlapping hyperfine structure should favour to the higher selectivity. Further, the resonant transitions selected from infrared or near infrared

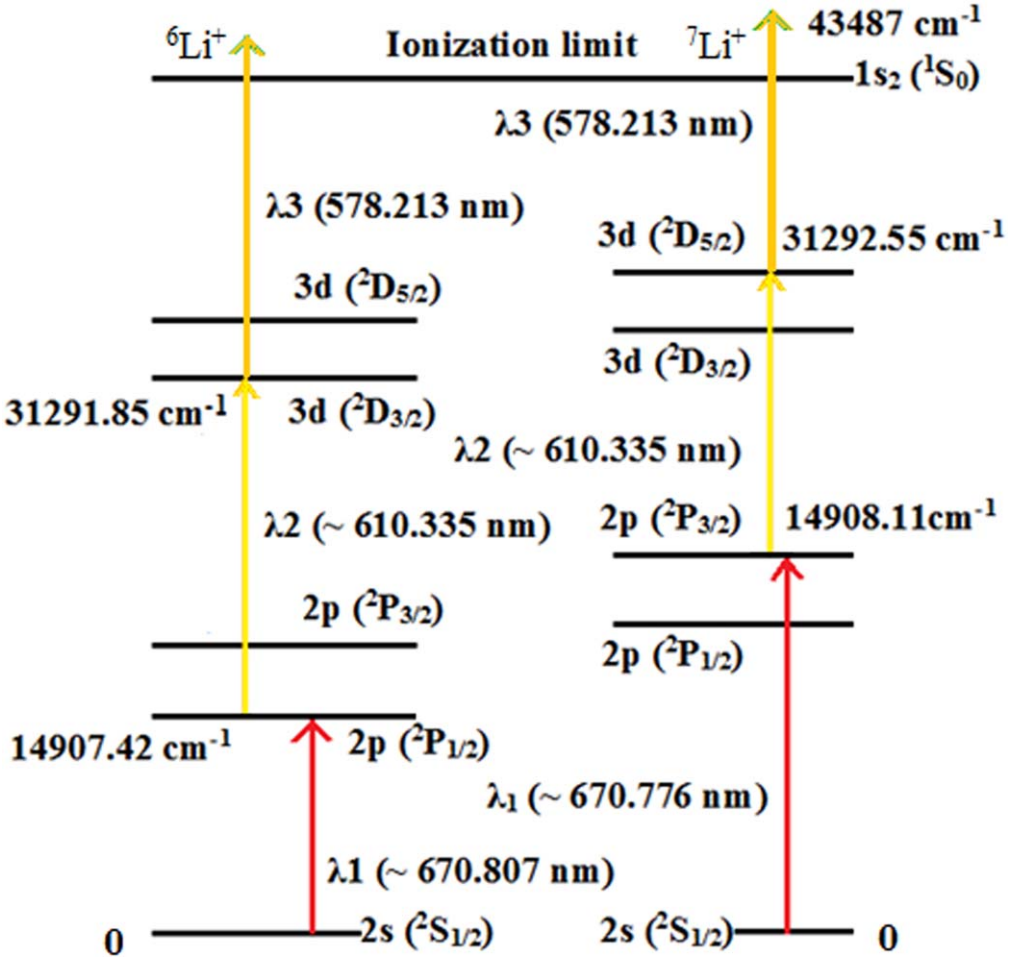

Figure 4. Three-color photoionization pathways for Li isotopes.

region having reduced Doppler width may effectively enhance the selectivity of process. When an atom is sequentially photo-ionized using three-step resonant ionization scheme as in present case of Li, the resulting total selectivity can be increased up to a value

$$S = S_1.S_2.S_3 \quad (5)$$

where S_i corresponds to selectivity of each i_{th} step. However, overall value of selectivity may be less if laser linewidth is larger than linewidth of the absorption transitions.

The Li isotopes have doublets and also the hyperfine fine structures (HFS) caused by non-zero nuclear spin (I = 1 for ^{6}Li and I = 3/2 for ^{7}Li). The HFS lines spacing is too small to be resolved by presently used dye lasers (B.W ~ 0.08 cm^{-1}), therefore these lines are not shown in energy level diagram. The energy separation between each isotope transition $^2S_{1/2} \rightarrow {}^2P_{1/2}$ and $^2S_{1/2} \rightarrow {}^2P_{3/2}$ called the D_1 and D_2 lines is around 0.0158 nm [28, 29]. The separation of D_1 and D_2 lines is comparable to the isotopic shift of 10.53 GHz for resonance line at 670.78 nm. It means $^2S_{1/2} \rightarrow {}^2P_{1/2}$ line of ^{7}Li nearly coincides with $^2S_{1/2} \rightarrow {}^2P_{3/2}$ line of ^{6}Li. Therefore, an extremely narrow linewidth of dye laser is required for isotopically selective excitation of such Li resonance levels. For higher isotope separation factor, it is advantageous to excite selectively either of two isotopes (^{6,7}Li) by tuning the dye laser wavelength to ^{7}Li ($^2S_{1/2} \rightarrow {}^2P_{3/2}$) or ^{6}Li ($^2S_{1/2} \rightarrow {}^2P_{1/2}$) resonance levels. As ionization potential (I.P) of Li is 5.39 eV [30] and the transition energy for 2p and 3d states are ~1.84 and 3.87 eV respectively, therefore population reached to the excited 3d levels can be ionized by photons with excitation wavelength shorter than 820 nm.

In a typical photoionization setup (figure 1), all the laser beams are set to interact with Li atoms simultaneously and high laser powers are required to obtain the high photoionization yield. However, for better efficiency high ionization yield at low laser powers is desirable in laser isotope separation [31]. There are few important parameters of atomic transitions such as the oscillator strength, lifetime and absorption cross-section that should be high in value to ascertain the suitability of atomic levels to make the photoionization more efficient [32]. Keeping all this in mind, a specific three-color scheme using three-step photoionization with two in close resonance is devised as shown in figure 4. For Li, all these parameters; the oscillator strength ($f_1 = 0.746$, $f_2 = 0.638$), lifetime ($\tau_1 = 27.1$ ns, $\tau_2 = 14.5$ ns) and absorption cross-section ($\sigma_{1,2} = \sim 10^{-12}$ to 10^{-11} cm^2) for both the first and second step transitions are well known and favorable [33–35]. The scheme for ^{7}Li photoionization has excitation process 2s $^2S_{1/2}$ (0 cm^{-1}) → 2p $^2P_{3/2}$ (14908.11 cm^{-1}) → 3d $^2D_{5/2}$ (31292.55 cm^{-1})

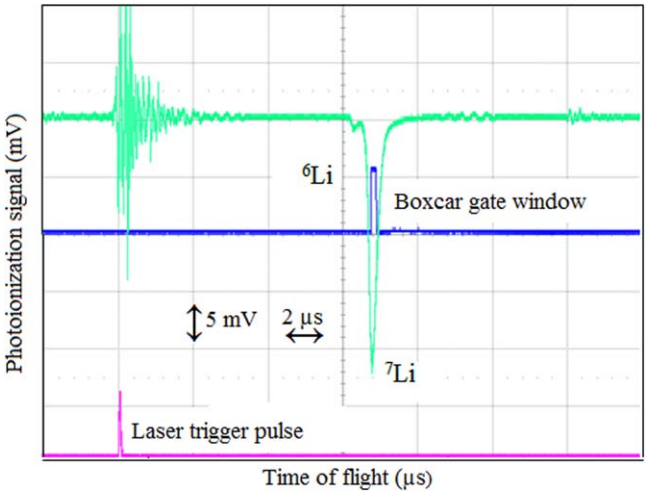

Figure 5. Lithium TOF mass-spectrum produced by three-color (λ_1: 670.765 nm, λ_2: 610.335 nm, λ_3: 578.213 nm) photo-ionization technique.

followed by third color non-resonant ionization by a photon of high energy (>1.5 eV) that can be obtained directly from CVL radiation (~578.2 nm). Similarly, for ^{6}Li, an excitation process 2s $^2S_{1/2}$ (0 cm^{-1}) → 2p $^2P_{1/2}$ (14907.42 cm^{-1}) → 3d $^2D_{3/2}$ (31291.85 cm^{-1}) followed by same non-resonant photo-ionization step is used. To improve the photoionization efficiency strong saturation of each steps transition are required. The possibility of transitions saturation with dye laser's available output power can be estimated by considering above mentioned transition parameters [35]. The average power of tunable dye lasers required to saturate the first and second step transitions are only few tens of mW at 6.5 kHz, however for third non-resonant step large power (typ. 5 Watts) is required at 578.2 nm radiation. The high laser power favors to higher photoionization efficiency, however it may subsequently deteriorate the selectivity [11, 27, 31] of process.

Earlier, Kramer *et al* [36] reported two-color resonant ionization for investigating the feasibility of Li single atom detection. Here, we extended the scheme to three-color/three-step photoionization using high repetition rate laser system and TOF mass-spectrometer. As the Li first and second step transition isotope-shifts are sufficiently large [29, 30], therefore high enrichment with large isotope separation factor can be anticipated from proposed scheme using the dye lasers with moderate output power and spectral bandwidth (~2.5 GHz). In third step no selectivity (S = 1) is expected as it uses the non-resonant ionization. As the experiment is carried out with high repetition rate (6.5 kHz) lasers at suitably high atom density (~10^{12} cm^{-3}), therefore overall high photo-ionization yield is also expected.

5. Results and discussion

A typical mass-spectrum of Li isotopes obtained using the above discussed three-colour photoionization scheme is shown in figure 5. On tuning dye laser-1 in the spectral range

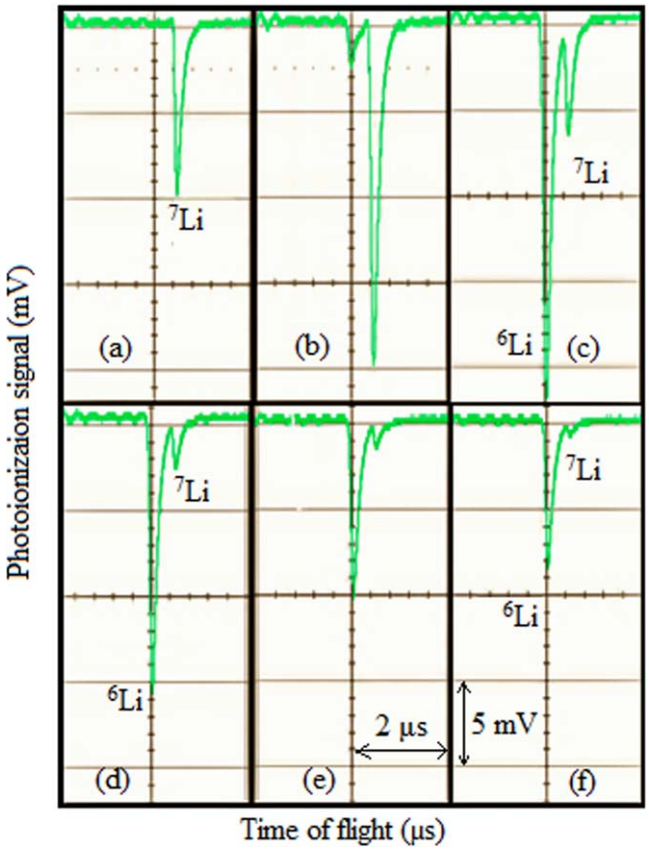

Figure 6. Effect of precise tuning of dye laser-1 on photoionization signals, in spectral range of 670.756 to 670.820 nm that corresponds to Li 1st transition ($^2S_{1/2} \rightarrow {}^2P_{1/2,3/2}$). Dye laser-2 wavelength for 2nd step transition ($^2P_{1/2} \rightarrow {}^2D_{3/2,5/2}$) is kept fixed at 610.335 nm. Ionizing laser pulse for 3rd non-resonant transition is at 578.213 nm wavelength. (typ. avg. powers are as 1st step: $P_1 = 42$ mW, 2nd step: $P_2 = 15$ mW and 3rd step: $P_3 = 6$ W).

of 670.756 to 670.820 nm, either one or both Li isotopes can be excited which results in proportionate photo-ion currents. When the first step excitation wavelength (λ_1) is varied from 670.750 to 670.850 nm, keeping the second step resonance transition wavelength (λ_2) fixed at 610.335 nm, the ion-current signals of ^{6}Li and ^{7}Li with varying signal peak heights are observed. The time of flight ^{6}Li and ^{7}Li lies in 6 to 7 micro-seconds range. The ^{6}Li peak appears ~400 ns before ^{7}Li. The reference laser excitation trigger pulse is used to measure the time of flight of respective isotopes. Maximum ion current signals are observed at coincidence of both the excitation and absorption centres of Li isotopes as the spectral width of dye laser radiation and transition absorption profile are ~0.04 Å and ~0.01Å respectively.

Few excerpts from recorded mass-spectrum obtained during the wavelength scanning are shown in figure 6. The excellent high selectivity is obtained for ^{7}Li corresponding to energy level resonance at 670.756 nm that may lead to its very high enrichment, see figure 6(a). On slight red shift in first step excitation wavelength, an additional weak signal just 400 ns before the strong ^{7}Li ion-signal appears at 670.792 nm which corresponds to ^{6}Li, see figure 6(b). Further on red shift, the strength of ^{6}Li ion-signal increases and surpass to ^{7}Li

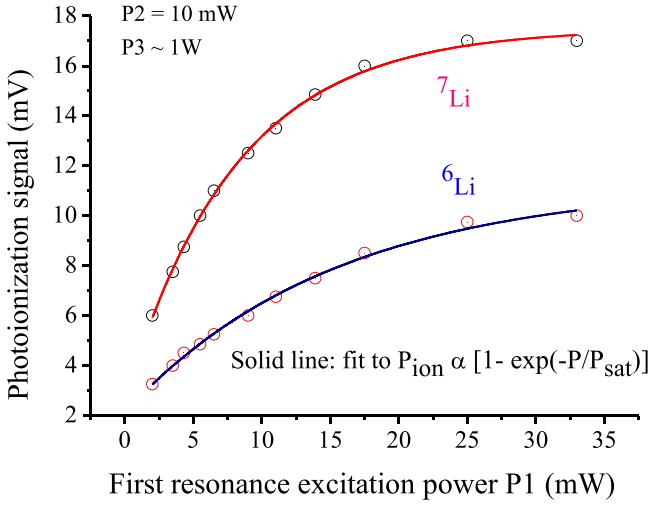

Figure 7. Laser power versus Li photo-ion yield for first-step transition.

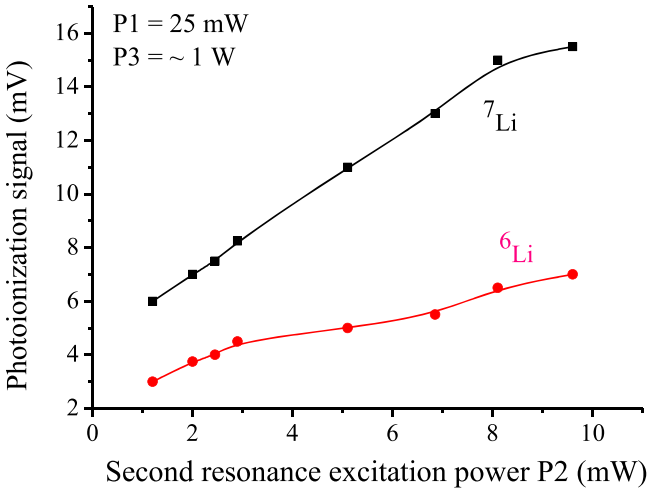

Figure 8. Laser power versus Li photo-ion yield for second-step transition.

signal significantly at 670.807 nm, see figure 6(c). At this wavelength, a noticeable ^{7}Li signal also occurs; however, only the ^{6}Li ($^{2}S_{1/2} \rightarrow {}^{2}P_{1/2}$) transition is excited. Probably, it is due to saturation broadening of the transitions at high laser powers used. For exploring the facts, dye laser power for both the 1st and 2nd resonant transitions are reduced considerably in steps using neutral density filters, see figures 6(d) to (f). Signals in figure 6(d) is recorded at (P_1: 20 mW, P_2: 15 mW, P_3: 6 W). Further, successive decrease in dye laser power (e.g. P_1: 5.5 mW, P_2: 5.2 mW, P_3: 6 W) leads to ionization signal of ^{6}Li only with a very small trace of ^{7}Li. This confirms that effects of laser power and/or transition saturation broadening affect the laser isotope separation process severely. It is observed that at high laser powers the yield of photoionization although is higher; however, the selectivity of process declines drastically.

The dependence of photo-ion signal on dye laser power for first transition in above discussed three-color photo-ionization scheme for both the isotopes is also investigated. The detailed analysis of transition saturation behaviour can be carried out from photo-ion signal recorded at different laser powers as shown in figure 7. An uncertainty (±5%) in the measurement of ion-signal is observed due to small (~3%) pulse to pulse variation in the laser's power. It is observed that ion-signal for both the isotopes increases first exponentially as the laser power increases and finally shows saturation at high laser powers. However, we tried to keep the laser powers small enough to avoid strong saturation of transitions and line broadening.

An exponential function of the type,

$$P_{ion}\alpha[1 - \exp(-P/P_{sat})] \quad (6)$$

describes and nicely fits the ion-signals that gives a slope of ion yield (P_{ion}) indicating the behaviour of transition saturation. It is observed that photoionization signal starts to saturate at 25 mW for both the isotopes for first-step transition. Similarly, dye laser power versus ion-yield for second-step transition is measured (see figure 8). For second-step, the ion-signal for both isotopes is found to increase almost linearly up to 8 mW and thereafter shows a trend of saturation at ~10 mW. To avoid strong transition saturation, the laser power (P2) is limited up to 10 mW. In this way, the photo-ion yield is well saturated close to 32 and 10 mW of dye lasers power for irradiation area (~2 mm^2) for the first and second steps, respectively. Similar values for Li are reported in literature [35]. Keeping dye laser powers fixed for both the first and second resonant steps at 25 mW and 10 mW respectively, the laser power for third non-resonant step is increased from 1 to 6 W and it is observed that ion-signal increased in a similar fashion up to 30 mV. Thereafter, the ion-signal remains nearly constant at higher laser power. However at large powers (>12 W), multiphoton ionization effects are observed on photo-ion signal. Thus, the saturation of transition in all steps can be used to monitor the performance of Li three-color photoionization and to check specifications for analysis.

Although, powers of the laser are optimized for first, second and third steps to obtain the high photoionization yield, however selectivity and hence the isotope abundance enhancement is observed to decline. For investigation of the facts, an experiment is carried out at two different laser excitation powers (figures 9 and 10) for first and second resonance steps, keeping the third-step laser power fixed. In figure 9(a), the ion-signal profile for ^{6}Li is measured by scanning the dye laser radiation frequency for first resonance transition at moderate higher laser power (i.e. P_1: 22 mW, P_2: 14 mW, P_3: 6W, Li temp: 505 °C). At these power levels the observed overall increase in homogeneous line broadening due to saturation effects can be related to

$$\Delta\nu(\mathrm{FWHM}) = \Delta\nu_N(1 + I/I_{sat})^{1/2} \quad (7)$$

where ($S_0 = I/I_{sat}$) is a saturation parameter. The I and I_{sat} are related to the laser powers P and P_{sat} for constant laser focus irradiation area (~2 mm^2). Although the term $\Delta\nu$ (FWHM) includes cumulative line broadening effects due to both the first and second resonance steps, however the value of saturation parameter ($S_0 \sim 5.81 \times 10^6$) is evaluated from measured width using natural linewidth ($2\pi\Delta\nu_N = A_{21} = 5.89$ MHz) of Li for the first transition

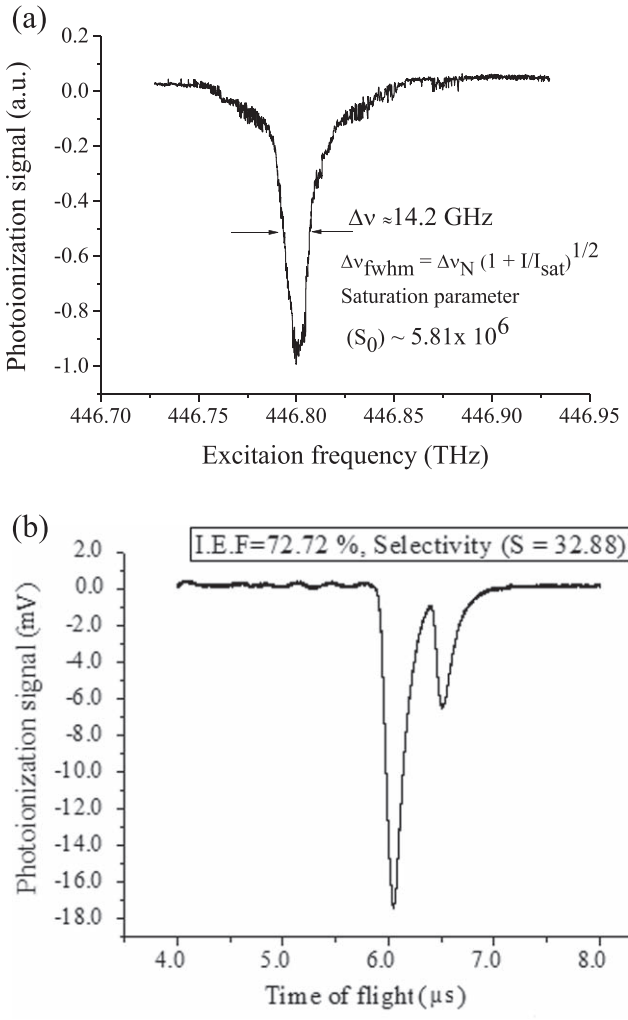

Figure 9. (a). Scanning for first-step transition at laser power (P_1: 22 mW, P_2: 14 mW, P_3: 6W). (b). TOF mass-spectrum at laser power (P_1: 22 mW, P_2: 14 mW, P_3: 6W).

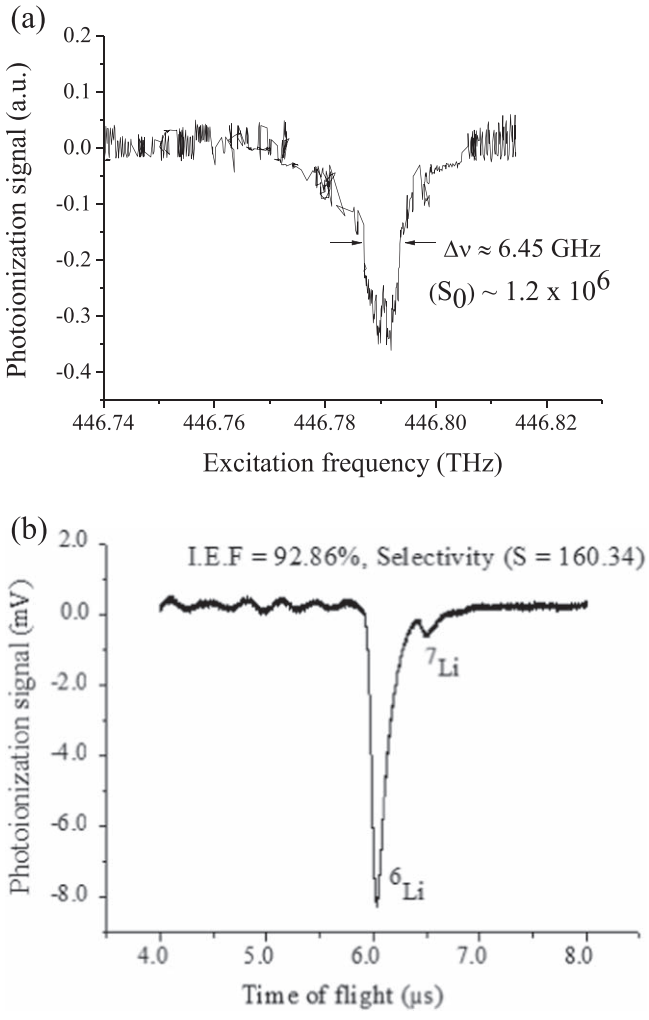

Figure 10. (a). Scanning for first-step transition at reduced laser power (P_1: 5.5 mW, P_2: 5.2 mW, P_3: 6W). (b). TOF mass-spectrum at reduced laser power (P_1: 5.5 mW, P_2: 5.2 mW, P_3: 6W).

only which sets the lower limit of transition line broadening. The Einstein coefficient (A_{21}) has been taken from [30]. At these laser power levels, overall isotope selectivity (S) from experimentally recorded TOF mass-spectrum, see figure 9(b), is determined as $[(^6Li/^7Li)_{product}/(^6Li/^7Li)_{feed} = 32.88]$. At this isotope selectivity, the isotope abundance enhancement factor (I.E.F) of 72.72% is obtained for ^{6}Li which is calculated as $[^6Li/(^6Li + ^7Li)] \times 100$.

In second case, when laser powers are reduced considerably the line broadening is minimized up to $\Delta\nu = 6.45$ GHz, see figure 10(a) which reduces the saturation parameter ($S_0 = 1.2 \times 10^6$) by a large factor (~5). At reduced laser power levels, see figure 10(b), the selectivity ($S = 160.34$) is observed to increase significantly and corresponding abundance I.E.F of 92.86% is acquired for ^{6}Li isotope. This shows that laser isotope separation by multi-step selective photoionization method is a suitable technique by which extreme high selectivity and hence high enrichment factor can be acquired with less complex setups.

The photoionization method can be also suitable for other elements also [37–39]. Although, overall efficiency of the method that include many processes such as generation of gas phase neutral atoms, laser ionization efficiency, ion beam extraction/transmission through mass-filter and ion-detection probability is low (~5%), however the selectivity and isotope purity obtained using this method is extremely high. The ion-yield and efficiency can be increased further by using very high repetition rate lasers and the multi-pass excitations.

6. Conclusion

The feasibility of Li isotope separation/enrichment by lasers using three-color isotope-selective photoionization in conjunction with time-of-flight mass-spectrometer is demonstrated. A system that includes high repetition rate copper vapour lasers, dye lasers, atomic beam vapour source and time-of-flight mass-spectrometer are developed for these studies. It is established that isotope selectivity and photoionization yield are the two important competing factors for ^{6}Li abundance enhancement that largely depends upon the photoionization scheme and laser system used. It is found that

Li atoms with natural isotopic abundance enhanced its ^{6}Li part up to over 92.86% by tuning the respective dye lasers to 2p($^{2}P_{1/2}$) and 3d($^{2}D_{3/2}$) resonance levels. Three-color photoionization [$^{2}S_{1/2} \rightarrow \xrightarrow{\sim 671\ \text{nm}} {}^{2}P_{1/2,3/2} \rightarrow \xrightarrow{\sim 610\ \text{nm}} {}^{2}D_{3/2,5/2} \xrightarrow{\sim 578\ \text{nm}} {}^{1}S_{0}$ (Li^{+})] with high repetition rate laser enables the high photoionization yield and large (>12 fold) enhancement in ^{6}Li abundance. The investigated three-color photoionization scheme with obtained high selectivity (∼160) may leads to high enrichment of ^{6}Li.

Acknowledgments

Authors are grateful to S V Nakhe and R Khare who inspired and extended the required help. The authors are thankful to C S Mandloi, L Chandervansi for their active support in TOF mass-spectrometer mechanical assembly, vacuum testing and related instrumentation. Authors are also thankful to U Kumbhkar for dye laser mechanical components fabrication and assembly and C T Sreerag for his support in the experiment.

ORCID iDs

V K Saini https://orcid.org/0000-0002-2120-4956
P K Saini https://orcid.org/0000-0002-8326-6917

References

[1] Giegerich T, Battes K, Schwenzer J C and Day C 2019 *Fusion Eng. and Design* **149** 111339
[2] Marcel D, Marco E, Martin W and Sascha N 2019 *RSC Adv.* **9** 12055
[3] Kanzaki Y, Suzuki N, Chitrakar R, Ohsaka T and Abe M 2002 *J. Phys. Chem.* B **106** 988
[4] Arisawa T, Maruyama Y, Suzuki Y and Shiba K 1982 *Appl. Phys.* B **28** 73
[5] Hurst G S and Payne M G 1988 *Principles and Applications of Resonance Ionization Spectroscopy* (Bristol: Adam Hilger)
[6] Letokhov V S 1987 *Laser Photoionization Spectroscopy* (New York: Academic)
[7] Tamura K, Oba M and Arisawa T 1993 *Appl. Optics* **32** 987
[8] Olivares I E and Durate A E 1999 *Appl. Optics* **38** 7481
[9] Myers E G, Murnick D E and Softky W R 1987 *App. Phys.* B **43** 247
[10] Karlov N V, Krynetskii B B, Mishin V A and Prokhorov A M 1978 *Appl. Optics* **17** 856
[11] Locke C R, Kobayashi T, Fujiwara T and Midorikawa K 2017 *Appl. Phys.* B **123** 240
[12] Il'n A M, Moschevikin A P and Khakhaev A D 1997 *Physica Scripta* **56** 587
[13] Saleem M, Hussain S, Rafiq M and Baig M A 2006 *J. Appl. Phys.* **100** 053111
[14] Saini V K, Talwar S, Subrahmanyam V V V and Dixit S K 2019 *Opt. and Laser Tech.* **111** 754
[15] Mittal J K, Bhadani P K, Singh B, Abhinandan L and Bhatnagar R 1988 *J. Phys. E: Sci. Instrum.* **21** 388
[16] Kumar J, Shukla P, Kumbhkar U, Prakash O, Khare R, Dixit S K and Mittal J K 2010 *National Laser Symp.-09, BARC Mumbai*
[17] Littman M G and Metcalf H J 1978 *Appl. Optics* **17** 2224
[18] Broyer M, Chevaleyre J, Delacretaz G and Woste L 1984 *Appl. Phys.* B **35** 31
[19] Khare R, Daulatabad S R, Vora H S and Bhatnagar R 1995 *Opt. Comm.* **114** 275
[20] Ramsey N 1969 *Molecular Beams* (London: Oxford Univ. Press)
[21] Talwar S, Subrahmanyam V V V, Saini V K, Sarangpani K K and Nakhe S V 2015 *Adv. Sci. Lett.* **21** 2556
[22] Gunther D and Hattendorf B 2005 *Trends in Anal. Chemistry* **24** 255
[23] Beer B and Heumann K G 1992 *Fresen. J. Anal. Chem.* **343** 741
[24] Williams M W, Beekman D W, Swan J B and Arakawa E T 1984 *Anal. Chem.* **56** 1348
[25] Betti M 2005 *Int. Journ. of Mass spectrometry* **242** 169
[26] Letokhov V S and Mishin V I 1979 *Opt. Comm.* **29** 168
[27] Karlov N V, Konev Y B and Prokhorov A M 1975 *Sov. J. Quant. Elect.* **5** 1336
[28] Moore C E 1971 *Atomic Energy Levels* (Washington DC: NSRDS-NBS)
[29] Walls J, Ashby R, Clarke J J, Lu B and Van Wijngaarden W A 2003 *Eur. Phys. J.* D **22** 159
[30] Herzberg G 1994 *Atomic Spectra and Atomic Structure* (New York: Dover Publications)
[31] Karlov N V and Prokhorov A M 1976 *Usp. Fiz. Nauk.* **118** 583
[32] Hurst G S, Pane M G, Kramer S D and Young J P 1979 *Rev. Mod. Phys.* **51** 767
[33] Yan Z C and Drake G W F 1995 *Phys. Rev.* A **52** 4316
[34] Heldt J and Leuchs G 1979 *Z. Phys.* A **291** 11
[35] Saloman E B 1993 *Spectrochim. Acta.* **48** **B** 1139
[36] Kramer S D, Young J P, Hurst G S and Payne M G 1979 *Opt. Comm.* **30** 47
[37] Pulhani A K, Gupta G P and Suri B M 2002 *J. Physics B: Atom. Mol. Opt. Physics* **35** 3677
[38] Hideaki N 2010 *J. Korean Phys. Soc.* 2010 **56** 190
[39] Cong R, Cheng Y, Yang J, Fan J, Yao G, Ji X, Zheng X and Cui Z *2009 J. Appl. Phys.* **106** 013103